Transceiver Design and Multi-hop D2D for UAV IoT Coverage in Disasters

Xiaonan Liu, Zan Li, *Senior Member, IEEE,* Nan Zhao, *Senior Member, IEEE,* Weixiao Meng, *Senior Member, IEEE,* Guan Gui, *Senior Member, IEEE,* Yunfei Chen, *Senior Member, IEEE,* and Fumiyuki Adachi, *Life Fellow, IEEE*

***Abstract*—When natural disasters strike, the coverage for Internet of Things (IoT) may be severely destroyed, due to the damaged communications infrastructure. Unmanned aerial vehicles (UAVs) can be exploited as flying base stations to provide emergency coverage for IoT, due to its mobility and flexibility. In this paper, we propose multi-antenna transceiver design and multi-hop device-to-device (D2D) communication to guarantee the reliable transmission and extend the UAV coverage for IoT in disasters. Firstly, multi-hop D2D links are established to extend the coverage of UAV emergency networks due to the constrained transmit power of the UAV. In particular, a shortest-path-routing algorithm is proposed to establish the D2D links rapidly with minimum nodes. The closed-form solutions for the number of hops and the outage probability are derived for the uplink and downlink. Secondly, the transceiver designs for the UAV uplink and downlink are studied to optimize the performance of UAV transmission. Due to the non-convexity of the problem, they are first transformed into convex ones and then, low-complexity algorithms are proposed to solve them efficiently. Simulation results show the performance improvement in the throughput and outage probability by the proposed schemes for UAV wireless coverage of IoT in disasters.**

***Index Terms*—Device to device, emergency wireless networks, internet of things, outage probability, transceiver design, unmanned aerial vehicle.**

I. Introduction

In natural disasters, rescue workers have to keep in touch with the control center and victims; while for the victims, they need to broadcast their locations and receive rescue information. Emergency communication network is a key factor for disaster relief [2]. However, communications infrastructure such as base stations (BSs) may be destroyed. This will cause serious delay to the rescue and recovery operations. To solve this problem, satellite and unmanned aerial vehicle (UAV)-based communications can be considered [3], [4]. In particular, UAVs can act as flying BSs to provide emergency wireless services in disaster affected areas for internet of things (IoT) [5]–[7].

UAV-aided networks can establish wireless interconnections quickly to achieve larger wireless coverage, which has attracted a lot of interests from both academia and industry [8]–[19]. In [8], three typical cases of UAV-aided wireless communications were summarized by Zeng *et al*., including UAV-aided ubiquitous coverage, UAV-aided relaying, and UAV-aided information dissemination. In [9], Lyu *et al*. proposed a spiral algorithm to minimize the number of required UAV-mounted mobile base stations to cover all the ground terminals. In [10], energy-efficient UAV communications were achieved through optimizing the UAV's trajectory by Zeng and Zhang. Zhao *et al*. proposed a blind beam tracking approach for Ka-band UAV-satellite communication system in [11], in which a hybrid large-scale antenna array is equipped at each UAV. In [12], Cheng did some research on the UAV trajectory at the edges of three adjacent cells to offload traffic for BSs. In [13], UAV assisted secure transmission for scalable videos in hyper-dense networks via caching was studied by Zhao *et al*. An anomaly detection system was developed by Lu *et al.* in [14], to prevent the motor of the drone from operating at abnormal temperatures. As effective means, the millimeter-wave and beamforming techniques [20] can also be adopted within the UAV-based networks [15]. Furthermore, a multi-objective path planning framework to explore a suitable path for a UAV operating in a dynamic urban environment was proposed by Yin *et al*. in [16].

Due to their excellent performances, UAVs have also been utilized in emergency wireless networks for disaster relief [21]–[24]. In [21], UAV-assisted disaster management applications were identified by Erdelj and Natalizio, and some related open research issues were discussed. In [22], a distributed and expansible architecture was proposed by Mase and Okada to provide message communication service to nodes in a wide disaster-affected area. Moreover, a deployment approach based on the combination of global and local search was exploited by Reina *et al*., to achieve optimal positioning of UAVs in disasters [23]. Meanwhile, in [24], UAV flying paths that can adapt to disaster condition and satisfy the energy constraint

This research was supported in part by the open research fund of State Key Laboratory of Integrated Services Networks under Grant ISN19-02, the Fundamental Research Funds for the Central Universities under DUT17JC43, the Xinghai Scholars Program, and the National Natural Science Foundation of China (NSFC) under Grant 61871065. Part of this work has been published in preliminary form in the Proceedings of IEEE/CIC 2018 [1]. *(Corresponding author: Nan Zhao.)*

X. Liu and N. Zhao are with the School of Inform. and Commun. Eng., Dalian University of Technology, Dalian, 116024, P. R. China, and also with the State Key Laboratory of Integrated Services Networks, Xidian University, Xi'an, 710071, P. R. China (email: liuxiaonan@mail.dlut.edu.cn, zhaonan@dlut.edu.cn).

Z. Li is with the State Key Laboratory of Integrated Services Networks, Xidian University, Xi'an 710071, P. R. China (Email: zanli@xidian.edu.cn).

W. Meng is with the Communication Research Center, Harbin Institute of Technology, Harbin 150001, P. R. China (e-mail: wxmeng@hit.edu.cn)

G. Gui is with Nanjing University of Posts and Telecommunications, Nanjing, Jiangsu, China (e-mail: guiguan@njupt.edu.cn).

Y. Chen is with the School of Engineering, University of Warwick, Coventry CV4 7AL, U.K. (e-mail: Yunfei.Chen@warwick.ac.uk).

F. Adachi is with the Research Organization of Electrical Communication, Tohoku University, Sendai 980-8577, Japan (e-mail: adachi@ecei.tohoku.ac.jp)

simultaneously were presented by Christy *et al*.

Although there are some advantages of using UAVs as flying BSs, many technical challenges still exist, including interference management, energy constraint and coverage limitation, *etc*. In particular, the disaster area may be very large, but the wireless coverage of UAV is limited due to insufficient battery. Thus, to overcome these challenges, multi-hop device-to-device (D2D) communications can be leveraged to assist the UAV to extend its wireless coverage effectively [25]–[30]. In a disastrous area that cannot be covered directly by the UAV, multi-hop D2D links can be established to relay the signals into its coverage area [31]. Thus, more mobile users can be served by the UAV. In recent years, plenty of research has been conducted on D2D communications [32]–[40]. In [32], a resource allocation problem was studied by Feng *et al*., to maximize the overall network throughput while guaranteeing the quality-of-service (QoS) requirements for D2D users. In [33], Lin *et al.* proposed a tractable hybrid network model to optimize the D2D spectrum sharing under a weighted proportional for utility function. In [34], the problem of energy-efficient uplink resource sharing over D2D multimedia communications underlaying small-cell networks with multiple mobile devices and cellular users was studied by Wu *et al*. Ban and Jung proposed two fundamental methods of D2D links scheduling in [35], i.e., centralized and distributed. In [36], Li *et al.* did some excellent research on the content caching in 5G cellular networks relying on social-aware D2D. A novel energy-efficient resource allocation algorithm was proposed by Zhou *et al*. in [37], via joint channel selection and power allocation. In [38], Ying *et al.* presented a social trust scheme that enhances the security of mobile social networks with mobile edge computing, caching and D2D. In [39], Mao *et al.* skillfully proved that the total degrees-of-freedom can achieve its optimum when the D2D links provided equal transmission rate as the original link. In [40], a heterogeneous framework was proposed by Cheng *et al.* to deliver smart grid data effectively, where D2D is leveraged to offload cellular networks.

In disasters, the wireless coverage of UAVs for IoT should be extended rapidly and effectively and thus, multi-hop D2D is leveraged in this paper to connect the outside mobile devices to the ones that lie in the coverage area. In this way, these devices can be linked to the UAV indirectly. In addition, to guarantee the reliable emergency communications, the transceiver of UAV is designed to optimize the spectrum efficiency in the uplink and downlink, respectively, with the advantages of multi-antenna resource at the UAV fully exploited [41]. The key contributions of this paper are summarized as follows.

- The disaster area is usually very large, however, the wireless coverage of a single UAV is limited due to the battery. Because of the limited resource in the emergency communication of disasters, we cannot deploy many UAVs to provide wireless coverage simultaneously. Thus, in this paper, we consider the UAV BS with fixed location, and the multi-hop D2D is leveraged to extend the coverage of UAV effectively.
- To the best of our knowledge, D2D and transceiver design have not been thoroughly studied in UAV-assisted emergency communications. In this paper, we utilize the multi-hop D2D and transceiver design to extend the wireless coverage and to guarantee the QoS of UAV communications for IoT in disasters.
- Multi-hop D2D is combined with UAV transmission in disasters, through which the mobile devices outside the coverage area can be connected to the UAV effectively. To minimize the number of hops, the shortest-path-routing (SPR) algorithm is designed to establish D2D links for emergency networks. The closed-form expressions of the number of hops and the outage probability are derived for the uplink and downlink.
- The multi-antenna resource of UAV is fully exploited with optimal transceiver design to guarantee reliable communications for both the UAV uplink and downlink. In particular, the transceiver design for the UAV downlink is non-convex, which is transformed into a convex one via convex approximation and solved by the second-order-cone programming (SOCP).

The rest of this paper is organized as follows. In Section II, the system model is presented. Outage probability for single-hop and multi-hop D2D in disasters are derived in Section III. The optimal transceiver designs for uplink and downlink transmission between the UAV and mobile devices are presented in Sections IV and V, respectively. In Section VI, simulation results are shown, followed by the conclusions and future work in Section VII.

Notation: $\mathbb{C}^{M\times N}$ denotes the space of complex $M \times N$ matrices. $\mathbf{A}^{\dagger}$ represents the conjugate transpose of matrix $\mathbf{A}$. $\mathcal{CN}(\mathbf{a}, \mathbf{A})$ stands for the complex Gaussian distribution with mean $\mathbf{a}$ and covariance matrix $\mathbf{A}$. $\mathcal{E}(\cdot)$ denotes expectation.

II. System Model

We consider a circular disaster area with radius $\bar{\mathcal{R}}$, in which BSs have been destroyed due to earthquake, flood, *etc*. Thus, the mobile devices cannot obtain wireless access service from the ground BSs. In this case, a UAV BS with M antennas is deployed to provide emergency coverage. Assume that the size of the UAV deployed in disasters is large enough, so that the antennas on it can be deemed as independent with each other. The mobiles are spatially distributed according to homogeneous Poisson Point Processes (PPP), as shown in Fig. 1. The UAV is located at the center of the disaster area with height H and can provide wireless service to several mobile devices simultaneously. The maximum effective transmission distance between an active device and the UAV can be denoted as

$$R_{UAV} = \frac{H}{\cos\varphi}, \tag{1}$$

where φ is the maximum angle between UAV and device. In addition, the mobile devices outside the coverage of UAV cannot connect to it directly, due to the limited transmit power of UAV and the device. In order to extend the coverage of UAV effectively, multi-hop D2D transmission is utilized to connect the devices outside with those inside. We assume that a D2D link can be established only when the distance between D2D transceivers is less than r. When the distance

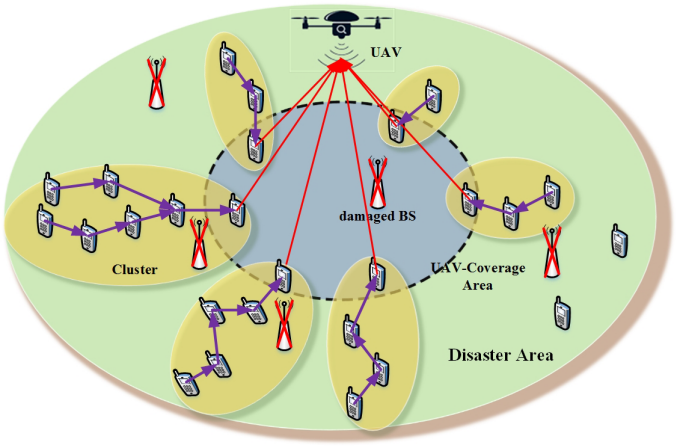

Fig. 1. Architecture of the UAV and D2D communication system.

between a mobile device and the UAV is larger than R_{UAV}, the interference from the device to the UAV can be neglected, due to the long distance and low transmit power of mobile devices. Meanwhile, we assume that all the D2D links operate in a half-duplex mode. To guarantee that the UAV can collect message from the active devices or send it to them in all directions, mobile devices are divided into $\hat{N}$ clusters, in which the lth cluster contains $N^{[l]}$ devices. The PPP density of D2D devices in the lth cluster is $\lambda_D^{[l]}$. In addition, we assume that the signal transmitted in a specific cluster will not be interfered by that from other clusters because those links are separated in a sufficiently long distance. Moreover, as for those devices that can communicate with the UAV directly in each cluster, some of them can be selected as source or destination nodes for multi-hop D2D links.

Thus, all the messages from the active devices can be delivered to the UAV through destination nodes in the uplink of multi-hop D2D, and the desired signal from the kth destination node at the UAV can be denoted as

$$y^{[k]} = \mathbf{u}^{[k]\dagger}\mathbf{h}^{[k]}x^{[k]} + \mathbf{u}^{[k]\dagger}\sum\nolimits_{j\in S_{DN},j\neq k}\mathbf{h}^{[j]}x^{[j]} + n_0, \quad (2)$$

where $\mathbf{h}^{[j]} = \sqrt{\rho_1 \hat{d}_{[j]}^{-\alpha_1}}\mathbf{h}_{up}^{[j]}$. $\mathbf{h}_{up}^{[j]} \in \mathbb{C}^{M\times 1}$ is the small-scale channel fading vector between the jth D2D destination node and the UAV. $\hat{d}_{[j]}$ is the distance between the jth D2D destination node and the UAV. ρ_1 and α_1 indicate the channel power gain at the reference distance and the path-loss exponent between the UAV and ground nodes, respectively. $\mathbf{u}^{[k]} \in \mathbb{C}^{M\times 1}$ denotes the decoding vector of the kth destination node at the UAV, with $\left\|\mathbf{u}^{[k]}\right\|^2 = 1$. $x^{[j]}$ is the signal transmitted by the jth D2D destination node. n_0 represents the additive white Gaussian noise (AWGN) satisfying distribution $\mathcal{CN}(0,\sigma^2)$ at the UAV. $\mathcal{S}_{DN}$ is the set that contains the D2D destination nodes in the uplink or source nodes in the downlink that communicate with the UAV, which should be less than or equal to $\hat{N}$. Then, the received signal-to-interference-plus-noise ratio (SINR) at the UAV from the kth destination node can be expressed as

$$\mathrm{SINR}_{UAV}^{[k]} = \frac{P^{[k]}\left|\mathbf{u}^{[k]\dagger}\mathbf{h}^{[k]}\right|^2}{\sum_{l\in\mathcal{S}_{DN},l\neq k}P^{[l]}\left|\mathbf{u}^{[k]\dagger}\mathbf{h}^{[l]}\right|^2 + \sigma^2}, \quad (3)$$

where $P^{[k]}$ is the transmit power of the kth D2D destination.

On the other hand, when the UAV delivers message to the source nodes in the downlink of multi-hop D2D, the desired signal at the kth D2D source node can be denoted as

$$\tilde{y}^{[k]} = \mathbf{g}^{[k]}\mathbf{v}^{[k]}\tilde{x}^{[k]} + \sum\nolimits_{i\in\mathcal{S}_{DN},j\neq k}\mathbf{g}^{[k]}\mathbf{v}^{[j]}\tilde{x}^{[j]} + n_0, \quad (4)$$

where $\mathbf{g}^{[k]} = \sqrt{\rho_1 \tilde{d}_{[k]}^{-\alpha_1}}\mathbf{g}_{down}^{[k]}$. $\mathbf{g}_{down}^{[k]} \in \mathbb{C}^{1\times M}$ is the small-scale channel fading vector between the UAV and the kth D2D source node. $\tilde{d}_{[k]}$ is the distance between the UAV and the kth D2D source node. $\mathbf{v}^{[k]} \in \mathbb{C}^{M\times 1}$ is the precoding vector of the kth D2D source node at the UAV, with $\sum_{k\in\mathcal{S}_{DN}}\left\|\mathbf{v}^{[k]}\right\|^2 \leq P_{sum}$, where P_{sum} is the transmit power constraint of the UAV. $\tilde{x}^{[k]}$ is the unit power signal transmitted from the UAV to the kth mobile device. Then, the received SINR at the kth mobile device can be calculated as

$$\mathrm{SINR}_{D}^{[k]} = \frac{\left|\mathbf{g}^{[k]}\mathbf{v}^{[k]}\right|^2}{\sum_{j\in\mathcal{S}_{DN},j\neq k}\left|\mathbf{g}^{[k]}\mathbf{v}^{[j]}\right|^2 + \sigma^2}. \quad (5)$$

Furthermore, in a specific uplink of multi-hop D2D, the desired signal at the kth D2D receiver can be presented as

$$\hat{y}^{[k]} = h^{[kk]}\hat{x}^{[k]} + \sum\nolimits_{j\in\mathcal{S}_I}h^{[kj]}\hat{x}^{[j]} + n_o, \quad (6)$$

where $h^{[kj]} = \sqrt{\rho_2 d_{[kj]}^{-\alpha_2}}h_{up}^{[kj]}$. $h_{up}^{[kj]}$ is the small-scale channel fading from the jth D2D transmitter to the kth D2D receiver in the uplink, which is identically and independently distributed (i.i.d.). $d_{[kj]}$ is the distance between the jth D2D transmitter to the kth D2D receiver. ρ_2 and α_2 indicate the channel power gain at the reference distance and the path-loss exponent between ground nodes, respectively. $\hat{x}^{[k]}$ is the signal transmitted by the kth D2D transmitter. $\mathcal{S}_I$ is the set that includes the D2D transmitters that may generate interference to the kth D2D receiver in the same cluster. Therefore, the SINR at the kth D2D receiver can be denoted as

$$\mathrm{SINR}_{UL}^{[k]} = \frac{\hat{P}^{[k]}g^{[kk]}}{\sum_{n\in\mathcal{S}_I}\hat{P}^{[n]}g^{[kn]} + \sigma^2}, \quad (7)$$

where $g^{[kk]} = \left|h^{[kk]}\right|^2$, and $\hat{P}^{[k]}$ is the transmit power of the kth D2D transmitter.

In addition, as for a specific downlink of multi-hop D2D, the UAV will communicate with its source node, and the desired signal at the kth D2D receiver can be denoted as

$$\bar{y}^{[k]} = \bar{h}^{[kk]}\bar{x}^{[k]} + \sum\nolimits_{j\in\mathcal{S}_I}\bar{h}^{[kj]}\bar{x}^{[j]} + \sum\nolimits_{i\in\mathcal{S}_{DN}}\bar{\mathbf{g}}^{[k]}\mathbf{v}^{[i]}\tilde{x}^{[i]} + n_o, \quad (8)$$

where $\bar{h}^{[kj]} = \sqrt{\rho_2 d_{[kj]}^{-\alpha_2}}\bar{h}_{down}^{[kj]}$. $\bar{h}_{down}^{[kj]}$ is the i.i.d. small-scale channel fading from the jth D2D transmitter to the kth D2D receiver in the downlink. Meanwhile, $\bar{\mathbf{g}}^{[k]} = \sqrt{\rho_1 \tilde{d}_{[k]}^{-\alpha_1}}\bar{\mathbf{g}}_{down}^{[k]}$. $\bar{\mathbf{g}}_{down}^{[k]} \in \mathbb{C}^{1\times M}$ is the small-scale channel fading vector between the UAV and the kth D2D receiver. $\bar{x}^{[k]}$ is the signal

transmitted by the kth D2D transmitter. $\bar{\mathcal{S}}_I$ is the set that includes the D2D transmitters that may generate interference to the kth D2D receiver in the same cluster. Thus, the SINR at the kth D2D receiver can be expressed as

$$\text{SINR}_{DL}^{[k]} = \frac{\hat{P}^{[k]}\bar{g}^{[kk]}}{\sum_{n\in\bar{\mathcal{S}}_I}\hat{P}^{[n]}\bar{g}^{[kn]} + \sum_{i\in\mathcal{S}_{DN}}\left|\bar{\mathbf{g}}^{[k]}\mathbf{v}^{[i]}\right|^2 + \sigma^2}, \tag{9}$$

where $\bar{g}^{[kk]} = \left|\bar{h}^{[kk]}\right|^2$.

In this paper, the shortest-path-routing (SPR) algorithm is first designed to establish the multi-hop D2D links to extend the wireless coverage of UAV with minimum number of hops, and the outage probability of multi-hop D2D links is analyzed. Then, the transceiver of the UAV is optimized to guarantee the emergency transmission performance of the UAV uplink and UAV downlink, respectively.

III. Multi-hop D2D Establishment

In this section, the SPR algorithm is designed to establish multi-hop D2D links effectively and rapidly with minimum number of hops. In addition, closed-form expressions of outage probability for multi-hop D2D are theoretically derived considering the interference from the UAV and other D2D links in the same cluster, for both uplink and downlink.

A. Outage Probability of a Single Hop

To derive the outage probability of multi-hop D2D, the expectation of outage probability for a specific single-hop D2D link is first obtained in this subsection. We consider two randomly located devices that wish to communicate with each other. The distance between these two devices is $\hat{r}$ ($\hat{r} \le r$), where r is the maximal distance between a specific D2D transmitter and its receiver. The outage probability of a D2D link can be defined as the probability that the average received SINR γ falls below a specific threshold ε, i.e., $\mathcal{P}(\gamma < \varepsilon)$. According to [42], the whole network can be divided into 2 tiers, i.e., the D2D and UAV tiers. As for the uplink of the multi-hop D2D links, the interference at the D2D receivers comes from the AWGN and nearby active D2D transmitters in the same cluster. Then, the probability of successful D2D transmission for the kth D2D receiver in the lth cluster with Rayleigh fading can be given by

$$\mathcal{P}_{UL}(\gamma_k > \varepsilon_l) = \exp\left[-\frac{\varepsilon_l}{\text{SNR}_{UL}} - \lambda_D^{[l]}\pi\hat{r}_{kk}^2 B_l(\varepsilon_l,\alpha)\right], \tag{10}$$

where $\text{SNR}_{UL} = \frac{\hat{P}^{[k]}g^{[kk]}}{\sigma^2}$, α is the path-loss exponent, $\hat{r}_{kk}$ is the distance between the kth D2D transmitter and its receiver, and $B_l(\varepsilon_l,\alpha)$ can be expressed as

$$B_l(\varepsilon_l,\alpha) = \varepsilon_l^{\frac{2}{\alpha}}\int_{(1/\varepsilon_l)^{2/\alpha}}^{\infty}\frac{1}{1+u^{\alpha/2}}du. \tag{11}$$

Moreover, as for the downlink of multi-hop D2D, the UAV will communicate with its source node, and the interference at the D2D receivers comes from the AWGN, the nearby active D2D transmitters in the same cluster, and the UAV. Then, the probability of successful D2D transmission for the kth D2D receiver in the lth cluster with Rayleigh fading can be expressed as

$$\mathcal{P}_{DL}(\gamma_k > \varepsilon_l) = \exp\left\{-\frac{\varepsilon_l}{\text{SNR}_{DL}} - \left[\lambda_D^{[l]} + \lambda_{UAV}\left(\frac{P_{sum}}{\hat{P}^{[k]}}\right)^{\frac{2}{\alpha}}\right]B_l(\varepsilon_l,\alpha)\pi\hat{r}_{kk}^2\right\}, \tag{12}$$

where $\text{SNR}_{DL} = \frac{\hat{P}^{[k]}\bar{g}^{[kk]}}{\sigma^2}$, λ_{UAV} is the density of UAV in the disaster area, which can be calculated as $1/(\pi(H\tan\varphi)^2)$. P_{sum} is the transmit power of the UAV. To be simplicity, we assume that AWGN can be ignored compared to the interference from the UAV and other active D2D devices in the same cluster, i.e., $\text{SNR}_{UL} \to \infty$ and $\text{SNR}_{DL} \to \infty$. Then, $\mathcal{P}_{UL}$ and $\mathcal{P}_{DL}$ can be rewritten as

$$\bar{\mathcal{P}}_{UL}(\gamma_k > \varepsilon_l) = \exp\left[-\lambda_D^{[l]}\pi\hat{r}_{kk}^2 B_l(\varepsilon_l,\alpha)\right], \tag{13}$$

and

$$\bar{\mathcal{P}}_{DL}(\gamma_k > \varepsilon_l) = \exp\left\{-\left[\lambda_D^{[l]} + \lambda_{UAV}\left(\frac{P_{sum}}{\hat{P}^{[k]}}\right)^{\frac{2}{\alpha}}\right]B_l(\varepsilon_l,\alpha)\,\pi\hat{r}_{kk}^2\right\}. \tag{14}$$

Thus, the outage probability of uplink and downlink for the kth D2D link in the lth cluster can be derived as

$$\mathcal{P}_{UL-out}^{[k]} = 1 - \bar{\mathcal{P}}_{UL}(\gamma_k > \varepsilon_l) = 1 - \exp\left[-\lambda_D^{[l]}\pi\hat{r}_{kk}^2 B_l(\varepsilon_l,\alpha)\right], \tag{15}$$

and

$$\mathcal{P}_{DL-out}^{[k]} = 1 - \bar{\mathcal{P}}_{DL}(\gamma_k > \varepsilon_l) = 1 - \exp\left\{-\left[\lambda_D^{[l]} + \lambda_{UAV}\left(\frac{P_{sum}}{\hat{P}^{[k]}}\right)^{\frac{2}{\alpha}}\right]B_l(\varepsilon_l,\alpha)\,\pi\hat{r}_{kk}^2\right\}. \tag{16}$$

In the lth cluster with $N^{[l]}$ devices and PPP density $\lambda_D^{[l]}$, the cumulative distribution function (CDF) of the distance $\hat{r}$ between the D2D transceiver can be denoted as

$$F_r(\hat{r}) = 1 - e^{-\left(N^{[l]}-1\right)\lambda_D^{[l]}\pi\hat{r}^2}. \tag{17}$$

Then, the probability density function (PDF) of the distance $\hat{r}$ of a D2D link can be presented as

$$f_r(\hat{r}) = \frac{\partial F_r(\hat{r})}{\partial\hat{r}} = 2\pi\hat{r}\left(N^{[l]}-1\right)\lambda_D^{[l]}e^{-\left(N^{[l]}-1\right)\lambda_D^{[l]}\pi\hat{r}^2}. \tag{18}$$

Thus, the average outage probability of uplink and downlink of the kth D2D link in the lth cluster can be expressed as

$$\begin{aligned}\mathcal{E}_{UL}^{[k]} &= 1 - \int_0^{+\infty}\bar{\mathcal{P}}_{UL}(\gamma_k > \varepsilon_l)f_r(\hat{r})d\hat{r} \\ &= 1 - \frac{N^{[l]}-1}{B_l(\varepsilon_l,\alpha) + \left(N^{[l]}-1\right)},\end{aligned} \tag{19}$$

and

$$\begin{aligned}\mathcal{E}_{DL}^{[k]} &= 1 - \int_0^{+\infty}\bar{\mathcal{P}}_{DL}(\gamma_k > \varepsilon_l)f_r(\hat{r})d\hat{r} \\ &= 1 - \frac{N^{[l]}-1}{B_l(\varepsilon_l,\alpha)\left[1+\frac{\lambda_{UAV}}{\lambda_D^{[l]}}\left(\frac{P_{sum}}{\hat{P}^{[k]}}\right)^{\frac{2}{\alpha}}\right] + \left(N^{[l]}-1\right)}.\end{aligned} \tag{20}$$

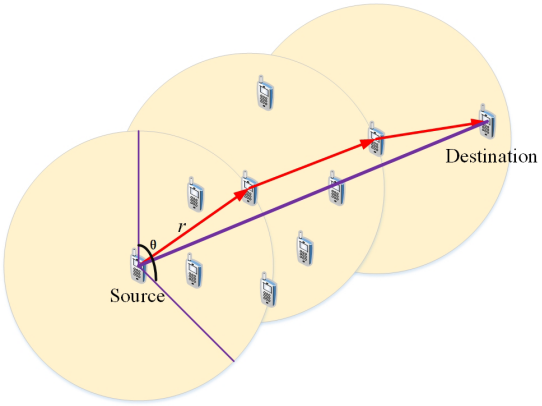

Fig. 2. Demonstration of the SPR algorithm.

B. Outage Probability of Multi-hop

In disasters, only a part of the mobile devices can be utilized to establish the multi-hop D2D links, due to the power limitation of each node and the shortage in power supply. Thus, to make full use of the resource and to save energy, the SPR algorithm is designed and utilized in disasters to establish the D2D links with minimum number of hops. In the algorithm, each active mobile device has knowledge of its own location and that of the destination node. With the help of the SPR algorithm, only the minimum number of hops is needed with relatively low outage probability and energy consumption. The SPR algorithm can be described step-by-step as follows, which is also shown in Fig. 2.

Step 1): In each cluster, a specific D2D transmitter can perform reliable transmission to a D2D receiver within the distance r, i.e., a D2D link only can be established effectively within a coverage radius r and a limited angle θ of the transmission direction.

Step 2): A device can be selected to perform as a relay node if it is much closer to the destination than all the other devices. Meanwhile, the selected device also needs to be closer to the line from the source to the destination.

Step 3): Due to the fact that several devices may want to send message to a certain selected node simultaneously, the device with the highest channel gain will transmit to that node, and others need to find some suboptimal ones. Nevertheless, if a certain device cannot find a proper relay node, it has to wait until a suitable node is available.

Step 4): Repeat steps 1) to 3) until the destination node can obtain all the messages.

Based on the SPR algorithm described above, the multi-hop D2D links can be established efficiently and rapidly with minimum number of hops. Due to the fact that different distributions may lead to different number of hops, to obtain the average outage probability of multi-hop D2D, the average number of hops is first derived. We assume that the reliable constraint of successful D2D transmission of uplink and downlink for each hop can be defined as ϕ_{UL} and ϕ_{DL}, respectively. Meanwhile, assume that the average transmit power allocated to each D2D node is $\hat{P}$. Then, we can obtain the average probability of successful transmission in the uplink and downlink for each hop as

$$\bar{\mathcal{P}}_{UL}(\gamma > \varepsilon) = \exp\left[-\lambda_D \pi \bar{r}_{UL}^2 B\left(\varepsilon, \alpha\right)\right] = \phi_{UL}, \tag{21}$$

and

$$\bar{\mathcal{P}}_{DL}(\gamma > \varepsilon) = \exp\left\{-\left[\lambda_D + \lambda_{UAV}\left(\frac{P_{sum}}{\hat{P}}\right)^{\frac{2}{\alpha}}\right] B(\varepsilon, \alpha)\, \pi \bar{r}_{DL}^2\right\} = \phi_{DL}, \tag{22}$$

where $\bar{r}_{UL}$ and $\bar{r}_{DL}$ are the average distances of a single D2D hop corresponding to the reliable constraint ϕ_{UL} and ϕ_{DL}, respectively. Then, we can derive $\bar{r}_{UL}$ and $\bar{r}_{DL}$ as

$$\bar{r}_{UL} = \sqrt{\frac{\ln(1/\phi_{UL})}{\lambda_D \pi B(\varepsilon, \alpha)}}, \tag{23}$$

and

$$\bar{r}_{DL} = \sqrt{\frac{\ln(1/\phi_{DL})}{\left[\lambda_D + \lambda_{UAV}\left(\frac{P_{sum}}{\hat{P}}\right)^{\frac{2}{\alpha}}\right] \pi B(\varepsilon, \alpha)}}. \tag{24}$$

According to (23) and (24), the average number of hops can be obtained as

$$J_{UL} = \left\lceil \frac{\mathcal{R}}{\bar{r}_{UL}} \right\rceil = \left\lceil \frac{\mathcal{R}\sqrt{\lambda_D \pi B(\varepsilon, \alpha)}}{\sqrt{\ln(1/\phi_{UL})}} \right\rceil, \tag{25}$$

and

$$J_{DL} = \left\lceil \frac{\mathcal{R}}{\bar{r}_{DL}} \right\rceil = \left\lceil \frac{\mathcal{R}\sqrt{\left[\lambda_D + \lambda_{UAV}\left(\frac{P_{sum}}{\hat{P}}\right)^{\frac{2}{\alpha}}\right] B(\varepsilon, \alpha)}}{\sqrt{\ln(1/\phi_{DL})}} \right\rceil, \tag{26}$$

where $\mathcal{R}$ is the distance between the source and destination of the multi-hop D2D link, and $\lceil . \rceil$ represents the ceiling function.

Therefore, based on the average outage probability for the kth D2D link of the lth cluster in (19) and (20), the average outage probability of the uplink and downlink of multi-hop D2D in the lth cluster can be obtained as a function of the successful probability for each hop as

$$\begin{aligned} \mathcal{P}_{D2D,out}^{UL} &= 1 - \prod_{k=1}^{J_{UL}} \left[1 - \hat{\mathcal{E}}_{UL}^{[k]}\right] \\ &= 1 - \prod_{k=1}^{J_{UL}} \int_0^{\bar{r}_{UL}} \mathcal{P}(\gamma_k > \varepsilon_l) f_r(\hat{r}) d\hat{r} \\ &= 1 - \prod_{k=1}^{J_{UL}} \phi_{UL}\left(1 - \exp\left(-\frac{\left(N^{[l]} - 1\right)\ln(1/\phi_{UL})}{B_l\left(\varepsilon_l, \alpha\right)}\right)\right), \end{aligned} \tag{27}$$

and

$$\begin{aligned}\mathcal{P}_{D2D,out}^{DL} &= 1-\prod_{k=1}^{J_{DL}}\left[1-\hat{\mathcal{E}}_{DL}^{[k]}\right] \\ &= 1-\prod_{k=1}^{J_{DL}}\int_0^{\bar{r}_{DL}}\mathcal{P}(\gamma_k>\varepsilon_l)f_r(\hat{r})d\hat{r} \\ &= 1-\prod_{k=1}^{J_{DL}}\phi_{DL}\left(1-\exp\left(-\frac{\left(N^{[l]}-1\right)\ln(1/\phi_{DL})}{\left[1+\frac{\lambda_{UAV}}{\lambda_D^{[l]}}\left(\frac{P_{sum}}{\hat{P}^{[k]}}\right)^{\frac{2}{\alpha}}\right]B_l(\varepsilon_l,\alpha)}\right)\right),\end{aligned} \tag{28}$$

where $\hat{\mathcal{E}}_{UL}^{[k]}$ and $\hat{\mathcal{E}}_{DL}^{[k]}$ are the expectation of the outage probability of the kth D2D link whose average distance are $\bar{r}_{UL}$ and $\bar{r}_{DL}$, respectively.

IV. Optimal Transceiver Design for UAV Uplink

In this section, we propose an optimal transceiver design scheme to maximize the sum rate of uplink transmission between the destination nodes of multi-hop D2D links and the UAV. The objective function of the problem is presented first, and then, an optimization algorithm based on the maximization of the received SINR is proposed to calculate its solutions effectively.

A. Problem Formulation

In the UAV uplink, the D2D destination nodes within the wireless coverage will deliver all the message from the active devices in the multi-hop D2D links of its own cluster to the UAV simultaneously, and thus interference will appear between these destination nodes at the UAV. To effectively manage the interference and improve the transmission performance, the decoding vectors of these destination nodes should be jointly designed.

For the kth destination node, the received rate at the UAV can be expressed as follows based on (3).

$$\begin{aligned}R^{[k]} &= \log_2\left(1+\text{SINR}_{UAV}^{[k]}\right) \\ &= \log_2\left(1+\frac{P\left|\mathbf{u}^{[k]\dagger}\mathbf{h}^{[k]}\right|^2}{\sum_{l\in\mathcal{S}_{DN},l\neq k}P\left|\mathbf{u}^{[k]\dagger}\mathbf{h}^{[l]}\right|^2+\sigma^2}\right).\end{aligned} \tag{29}$$

In (29), the transmit power of all the destination nodes is assumed to be the same, i.e., $P^{[k]}=P, \forall k\in\mathcal{S}_{DN}$. This is due to the fact that it is difficult to perform power allocation at the destination nodes in disasters. Especially, if the transmit power is centrally controlled, the power consumption of the limited-battery UAV will increase by transmitting additional control signals. If the transmit power is controlled in a distributed manner, the channel state information (CSI) of all the other destinations should be fed back from UAV to each node, which will also cause high power consumption of the UAV.

To maximize the sum rate at the UAV with the minimum rate of each node guaranteed, (P1) can be presented as

$$\begin{aligned}(P1)\ \max_{\mathbf{u}^{[k]}}&\sum\nolimits_{k\in\mathcal{S}_{DN}}R^{[k]} \\ s.t.\quad&\left\|\mathbf{u}^{[k]}\right\|^2=1,\quad\forall k\in\mathcal{S}_{DN}, \\ &R^{[k]}\geq\delta^{[k]},\quad\forall k\in\mathcal{S}_{DN},\end{aligned} \tag{30}$$

where $\delta^{[k]}$ is rate threshold of the kth destination node that should be guaranteed.

From (P1), we can see that it is non-convex, which is difficult to solve. In the next subsection, we propose an effective optimization algorithm to calculate its solutions through maximizing the SINR.

B. Optimization Algorithm for (30)

(P1) can be reformulated through introducing an auxiliary variable as

$$\begin{aligned}\max_{\mathbf{u}^{[k]}}&\sum\nolimits_{k\in\mathcal{S}_{DN}}\left(\log_2\left(1+\text{SINR}_{UAV}^{[k]}\right)=\log_2(s_k)\right) \\ s.t.\quad&\left\|\mathbf{u}^{[k]}\right\|^2=1,\quad\forall k\in\mathcal{S}_{DN}, \\ &\text{SINR}_{UAV}^{[k]}\geq s_k-1=\bar{s_k},\quad\forall k\in\mathcal{S}_{DN},\end{aligned} \tag{31}$$

where s_k is the SINR corresponding to the threshold $\delta^{[k]}$ of the kth destination node. Obviously, (31) can be changed into

$$\begin{aligned}\max_{\mathbf{u}^{[k]}}&\prod_{k\in\mathcal{S}_{DN}}s_k \\ s.t.\quad&\left\|\mathbf{u}^{[k]}\right\|^2=1,\quad\forall k\in\mathcal{S}_{DN}, \\ &\frac{P\left|\mathbf{u}^{[k]\dagger}\mathbf{h}^{[k]}\right|^2}{\sum_{l\in\mathcal{S}_{DN},l\neq k}P\left|\mathbf{u}^{[k]\dagger}\mathbf{h}^{[l]}\right|^2+\sigma^2}\geq\bar{s_k},\ \forall k\in\mathcal{S}_{DN}.\end{aligned} \tag{32}$$

Assume that the number of active users in set $\mathcal{S}_{DN}$ is $\hat{N}$. To solve the problem (32), we can decompose the problem into $\hat{N}$ feasible subproblems, and the kth corresponding subproblem can be expressed as

$$\begin{aligned}\max_{\mathbf{u}^{[k]}}&s_k \\ s.t.\quad&\left\|\mathbf{u}^{[k]}\right\|^2=1,\quad\forall k\in\mathcal{S}_{DN}, \\ &\frac{P\left|\mathbf{u}^{[k]\dagger}\mathbf{h}^{[k]}\right|^2}{\sum_{l\in\mathcal{S}_{DN},l\neq k}P\left|\mathbf{u}^{[k]\dagger}\mathbf{h}^{[l]}\right|^2+\sigma^2}\geq\bar{s_k},\ \forall k\in\mathcal{S}_{DN}.\end{aligned} \tag{33}$$

From (33), we can know that the kth subproblem is equivalent to the problem in [43], which aims to maximize $\text{SINR}_{UAV}^{[k]}$ with respect to $\mathbf{u}^{[k]}$. The received SINR at the UAV from the kth destination node in (3) can be rewritten as

$$\text{SINR}_{UAV}^{[k]}=\frac{P\mathbf{u}^{[k]\dagger}\mathbf{h}^{[k]}\mathbf{h}^{[k]\dagger}\mathbf{u}^{[k]}}{\mathbf{u}^{[k]\dagger}\mathbf{Q}^{[k]}\mathbf{u}^{[k]}},\forall k\in\mathcal{S}_{DN}, \tag{34}$$

where

$$\mathbf{Q}^{[k]}=\sum\nolimits_{l\in\mathcal{S}_{DN},l\neq k}P\mathbf{h}^{[l]}\mathbf{h}^{[l]\dagger}+\sigma^2\mathbf{I}^{[k]}. \tag{35}$$

Then, the optimal solution of $\mathbf{u}^{[k]}$ that maximizes $\text{SINR}_{UAV}^{[k]}$

can be derived as

$$\mathbf{u}^{[k]\star} = \frac{\left(\mathbf{Q}^{[k]}\right)^{-1}\mathbf{h}^{[k]}}{\left\|\left(\mathbf{Q}^{[k]}\right)^{-1}\mathbf{h}^{[k]}\right\|},\ \forall k \in \mathcal{S}_{DN}. \tag{36}$$

Thus, (P1) in (30) can be solved by calculating the decoding vector in (36) $\hat{N}$ times, with relatively low computational complexity. In addition, the interference is not eliminated perfectly at the UAV according to (30), and the sum rate is maximized instead. Nevertheless, the reliable performance can be guaranteed in (30), only when enough antennas to perform perfect interference elimination are equipped at the UAV, i.e., $M \geq \hat{N}$.

When considering the more complex UAV downlink, the precoding vectors should be jointly optimized with transmit power considered, which will be presented in the next section.

V. Optimal Transceiver Design for UAV Downlink

In this section, we propose an optimal transceiver design scheme to maximize the sum rate of the downlink transmission between the UAV and the source nodes of multi-hop D2D links. The objective function of the problem is presented first, and then, the suboptimal solutions can be calculated based on SOCP.

A. Problem Formulation

In the UAV downlink, the UAV will deliver the message to all the source nodes of multi-hop D2D links simultaneously, and thus interference will appear between these source nodes. To handle the interference effectively, the precoding vectors for these source nodes at the UAV should be jointly designed.

For the kth source node, its received rate from the UAV can be expressed as follows based on (5).

$$\begin{aligned} R_D^{[k]} &= \log_2\left(1+\mathrm{SINR}_D^{[k]}\right) \\ &= \log_2\left(1+\frac{\left|\mathbf{g}^{[k]}\mathbf{v}^{[k]}\right|^2}{\sum_{j\in\mathcal{S}_{DN},j\neq k}\left|\mathbf{g}^{[k]}\mathbf{v}^{[j]}\right|^2+\sigma^2}\right). \end{aligned} \tag{37}$$

To maximize the sum rate of all the D2D source nodes, with the minimum rate of each node and transmit power constraint of UAV guaranteed, the optimization problem (P2) can be expressed as

$$(P2)\ \max_{\mathbf{v}^{[k]}}\ \sum\nolimits_{k\in\mathcal{S}_{DN}} R_D^{[k]} \tag{38a}$$

$$s.t.\ \ R_D^{[k]} \geq \tilde{\delta}^{[k]},\quad \forall k \in \mathcal{S}_{DN}, \tag{38b}$$

$$\sum\nolimits_{k\in\mathcal{S}_{DN}}\left\|\mathbf{v}^{[k]}\right\|^2 \leq P_{sum},\ \forall k \in \mathcal{S}_{DN}, \tag{38c}$$

where $\tilde{\delta}^{[k]}$ is the rate threshold of the kth source node that should be guaranteed, and P_{sum} denotes the transmit power constraint of the UAV.

From the problem (P2), we can know that (38) is non-convex and its global optimum is difficult to achieve. In the next subsection, we first transform it into a convex one through convex approximation, and then, derive its suboptimal solutions.

B. Optimization Algorithm for (38)

In this section, an optimization algorithm is proposed to derive the suboptimal solution of problem (P2). First, (P2) can be reformulated through introducing an auxiliary variable as

$$(P2)\ \max_{\mathbf{v}^{[k]},\tilde{s}_k}\ \sum_{k\in\mathcal{S}_{DN}}\log_2(\tilde{s}_k) \tag{39a}$$

$$s.t.\ \ \frac{\left|\mathbf{g}^{[k]}\mathbf{v}^{[k]}\right|^2}{\sum\limits_{j\in\mathcal{S}_{DN},j\neq k}\left|\mathbf{g}^{[k]}\mathbf{v}^{[j]}\right|^2+\sigma^2} \geq \tilde{s}_k - 1, \tag{39b}$$

$$\sum_{k\in\mathcal{S}_{DN}}\left\|\mathbf{v}^{[k]}\right\|^2 \leq P_{sum}, \tag{39c}$$

where $\tilde{s}_k$ is the SINR corresponding to the rate threshold $\tilde{\delta}^{[k]}$ of the kth source node.

Obviously, (39) is equivalent to

$$\max_{\mathbf{v}^{[k]},\tilde{s}_k}\ \prod_{k\in\mathcal{S}_{DN}}\tilde{s}_k \tag{40a}$$

$$s.t.\ \ \frac{\left|\mathbf{g}^{[k]}\mathbf{v}^{[k]}\right|^2}{\tilde{s}_k-1} \geq \sum_{j\in\mathcal{S}_{DN},j\neq k}\left|\mathbf{g}^{[k]}\mathbf{v}^{[j]}\right|^2+\sigma^2, \tag{40b}$$

$$\sum_{k\in\mathcal{S}_{DN}}\left\|\mathbf{v}^{[k]}\right\|^2 \leq P_{sum}. \tag{40c}$$

Although $\mathcal{G}_1 = \frac{\left|\mathbf{g}^{[k]}\mathbf{v}^{[k]}\right|^2}{\tilde{s}_k-1}$ and $\mathcal{G}_2 = \sum\limits_{j\in\mathcal{S}_{DN},j\neq k}\left|\mathbf{g}^{[k]}\mathbf{v}^{[j]}\right|^2+\sigma^2$ in (40b) are convex, $\mathcal{G}_1-\mathcal{G}_2 \geq 0$ is not. Thus, we can know that (40b) is still not convex in the form of $\mathcal{G}_1 \geq \mathcal{G}_2$. Nevertheless, based on the constrained concave convex procedure in [44], the function $\mathcal{G}_1$ in (40b) can be expressed with its corresponding first-order Taylor expansion approximately. Thus, these constraints can be converted into convex ones. Before introducing the conversion, Lemma 1 is presented as follows.

Lemma 1: Consider a quadratic-over-linear function as

$$\mathcal{F}(\mathbf{x},z) = \frac{\mathbf{b}\mathbf{x}\mathbf{x}^\dagger\mathbf{b}^\dagger}{z-c}, \tag{41}$$

in which $\mathbf{B}=\mathbf{b}\mathbf{b}^\dagger \succeq 0$ and c is a constant. We can obtain the first-order Taylor expansion of (41) as follows.

$$\mathcal{Q}(\mathbf{x},z,\bar{\mathbf{x}},\bar{z}) = \frac{2Re\left(\bar{\mathbf{x}}^\dagger\mathbf{b}\mathbf{b}^\dagger\mathbf{x}\right)}{\bar{z}-c} - \frac{\bar{\mathbf{x}}^\dagger\mathbf{b}\mathbf{b}^\dagger\bar{\mathbf{x}}}{(\bar{z}-c)^2}(z-c), \tag{42}$$

which can meet the condition of $\mathcal{F}(\mathbf{x},z) \geq \mathcal{Q}(\mathbf{x},z,\bar{\mathbf{x}},\bar{z})$.

Proof: The first-order Taylor expansion of $\mathcal{F}(\mathbf{x},z)$ can be obtained as

$$\begin{aligned} \mathcal{Q}(\mathbf{x},z,\bar{\mathbf{x}},\bar{z}) =& \mathcal{F}(\bar{\mathbf{x}},\bar{z}) + \partial_z\mathcal{F}|_{(\bar{\mathbf{x}},\bar{z})}(z-\bar{z}) + \partial_{\mathbf{x}}\mathcal{F}|_{(\bar{\mathbf{x}},\bar{z})}(\mathbf{x}-\bar{\mathbf{x}}) \\ =& \frac{\mathbf{b}\bar{\mathbf{x}}\bar{\mathbf{x}}^\dagger\mathbf{b}^\dagger}{\bar{z}-c} - \frac{\mathbf{b}\bar{\mathbf{x}}\bar{\mathbf{x}}^\dagger\mathbf{b}^\dagger}{(\bar{z}-c)^2}(z-\bar{z}) + \frac{2\bar{\mathbf{x}}^\dagger\mathbf{b}\mathbf{b}^\dagger}{\bar{z}-c}(\mathbf{x}-\bar{\mathbf{x}}). \end{aligned} \tag{43}$$

Owing to the equality $\mathbf{b}\bar{\mathbf{x}}\bar{\mathbf{x}}^\dagger\mathbf{b}^\dagger = \bar{\mathbf{x}}^\dagger\mathbf{b}\mathbf{b}^\dagger\bar{\mathbf{x}}$, (43) can be rewritten

$$\max_{\mathbf{v}^{[k]},\tilde{s}_k} \; t^{(0)} \tag{48a}$$

$$s.t. \quad \left\| \left[2t_i^{(C-1)}, (\tilde{s}_{2i-1} - \tilde{s}_{2i}) \right]^\dagger \right\| \leq \tilde{s}_{2i-1} + \tilde{s}_{2i}, i = 1, 2, ..., 2^{C-1}, \tag{48b}$$

$$\left\| \left[2t_i^{(C-2)}, \left(t_{2i-1}^{(C-1)} - t_{2i}^{(C-1)} \right) \right]^\dagger \right\| \leq t_{2i-1}^{(C-1)} + t_{2i}^{(C-1)}, i = 1, 2, ..., 2^{C-2}, \tag{48c}$$

$$\cdots\cdots$$

$$\left\| \left[2t^{(0)}, \left(t_1^{(1)} - t_2^{(1)} \right) \right]^\dagger \right\| \leq t_1^{(1)} + t_2^{(1)}, i = 1, \tag{48d}$$

$$\left\| \left[2\mathbf{v}^{[1]\dagger}\mathbf{g}^{[k]\dagger}, \ldots, 2\mathbf{v}^{[j]\dagger}\mathbf{g}^{[k]\dagger}, \ldots, 2\mathbf{v}^{[\hat{N}]\dagger}\mathbf{g}^{[k]\dagger}, \Gamma_{1k} - 1 \right]^\dagger \right\|^2 \leq \Gamma_{1k} + 1, \; \forall k \in \mathcal{S}_{DN}, \; j \neq k, \tag{48e}$$

$$\left\| \left[\mathbf{v}^{[1]\dagger}, \mathbf{v}^{[2]\dagger} \ldots, \mathbf{v}^{[\hat{N}]\dagger} \right]^\dagger \right\|^2 \leq \sqrt{P_{sum}}. \tag{48f}$$

as

$$\mathcal{Q}(\mathbf{x}, z, \bar{\mathbf{x}}, \bar{z}) = \frac{2\bar{\mathbf{x}}^\dagger \mathbf{b}\mathbf{b}^\dagger \mathbf{x}}{\bar{z} - c} - \frac{\bar{\mathbf{x}}^\dagger \mathbf{b}\mathbf{b}^\dagger \bar{\mathbf{x}}}{(\bar{z} - c)^2} (z - c). \tag{44}$$

For easy calculation, $\bar{\mathbf{x}}^\dagger \mathbf{b}\mathbf{b}^\dagger \mathbf{x}$ can be replaced by $Re(\bar{\mathbf{x}}^\dagger \mathbf{b}\mathbf{b}^\dagger \mathbf{x})$ approximately, and thus, we can change the first-order Taylor expansion of (44) into

$$\mathcal{Q}(\mathbf{x}, z, \bar{\mathbf{x}}, \bar{z}) = \frac{2Re(\bar{\mathbf{x}}^\dagger \mathbf{b}\mathbf{b}^\dagger \mathbf{x})}{\bar{z} - c} - \frac{\bar{\mathbf{x}}^\dagger \mathbf{b}\mathbf{b}^\dagger \bar{\mathbf{x}}}{(\bar{z} - c)^2} (z - c). \tag{45}$$

Therefore, we can conclude that $\mathcal{F}(\mathbf{x}, z) \geq \mathcal{Q}(\mathbf{x}, z, \bar{\mathbf{x}}, \bar{z})$, according to the first-order convex condition. ■

Based on Lemma 1, as for (40b), we can define

$$\mathcal{F}_1 \left(\mathbf{v}^{[k]}, \tilde{s}_k \right) = \frac{\mathbf{g}^{[k]} \mathbf{v}^{[k]} \mathbf{v}^{[k]\dagger} \mathbf{g}^{[k]\dagger}}{\tilde{s}_k - 1}. \tag{46}$$

The first-order Taylor expansion of (46) at a specific point $\left(\bar{\mathbf{v}}^{[k]}, \tilde{\bar{s}}_k \right)$ can be approximated of as

$$\mathcal{Q}_1 \left(\mathbf{v}^{[k]}, \tilde{s}_k, \bar{\mathbf{v}}^{[k]}, \tilde{\bar{s}}_k \right) = \frac{2Re \left(\bar{\mathbf{v}}^{[k]\dagger} \mathbf{g}^{[k]} \mathbf{g}^{[k]\dagger} \mathbf{v}^{[k]} \right)}{\tilde{\bar{s}}_k - 1} - \frac{\bar{\mathbf{v}}^{[k]\dagger} \mathbf{g}^{[k]} \mathbf{g}^{[k]\dagger} \bar{\mathbf{v}}^{[k]}}{\left(\tilde{\bar{s}}_k - 1 \right)^2} (\tilde{s}_k - 1). \tag{47}$$

Based on the above derivation, we can replace the lower bound in (47) in the left side of (40b). Then, the constraint of (40b) can be changed into a convex one. In addition, we can observe that (40a) is expressed as a product of $\tilde{s}_k$, which can also be changed into the form of SOCP to further reduce its complexity. Therefore, we first review a lemma in [45] as follows.

Lemma 2: The hyperbolic constraints of a convex problem can be expressed as SOCPs via the following fact. $d^2 \leq ef, e \geq 0, f \geq 0 \Longleftrightarrow \left\| [2d, e - f]^\dagger \right\| \leq e + f.$ ■

Thus, based on the result of Lemma 2, we can change (40a) into a series of constraints (48a)-(48d) in the form of second-order cone (SOC). Accordingly, with all the approximations and transformations derived above, we can rewritten (40) as a SOCP problem, which is presented as (48), in which Γ_{1k} can be expressed as

$$\Gamma_{1k} = \mathcal{Q}_1 \left(\mathbf{v}^{[k]}, \tilde{s}_k, \bar{\mathbf{v}}^{[k]}, \tilde{\bar{s}}_k \right) - \sigma^2. \tag{49}$$

In (38b), $C = \left\lceil \log_2 \hat{N} \right\rceil$, and let $\tilde{s}_j = 1$ for the case of $\hat{N} < 2^C$, where $j = \left\{ \hat{N} + 1, \ldots, 2^{\left\lceil \log_2 \hat{N} \right\rceil} \right\}$. Then, $\left(\bar{\mathbf{v}}^{[k]}, \tilde{\bar{s}}_k \right)$ are set as the initial values, and thus, the solutions to the SOCP problem in (38) can be calculated via existing toolboxes. Note that, we can obtain only a feasible solution of $\mathbf{v}^{[k]}$ via solving (38), and the suboptimal solution $\mathbf{v}^{[k]*}$ can be calculated by iteration, which will be illustrated in the next subsection.

C. Proposed SOCP Algorithm

According to the results in Subsection V-B, an optimization algorithm with the help of SOCP is proposed to obtain the solutions to (38) in the optimal transceiver design scheme for UAV downlink, as summarized in Algorithm 1. According to [44], Algorithm 1 is convergent. When the proper initial values are set, we can always obtain a local suboptimal solution to (38).

Algorithm 1 SOCP Algorithm for (38)

1: Set $\mathcal{N}$ as the maximum iterations. Determine the feasible values of $(\bar{\mathbf{v}}^{[k]}, \tilde{\bar{s}}_k)$ for (48) randomly .
2: **Repeat**
3: Solve (48) via existing toolboxes, and thus, calculate the solutions of $(\mathbf{v}^{[k]*}, \tilde{s}_k^*)$.
5: Replace $(\bar{\mathbf{v}}^{[k]}, \tilde{\bar{s}}_k)$ with $(\mathbf{v}^{[k]*}, \tilde{s}_k^*)$.
6: $n = n + 1$.
7: **Until** $n = \mathcal{N}$.
8: Output: $\mathbf{v}^{[k]*}$.

In addition, the interference is not perfectly zero-forced at each device by the UAV according to (38), and the sum rate is maximized instead. Nevertheless, the reliable performance can

be guaranteed in (38), only when enough antennas to perform perfect zero-forcing are equipped at the UAV, i.e., $M \geq \hat{N}$.

VI. Simulation Results and Discussion

In this section, the performances of the proposed schemes are simulated. Consider a UAV aided wireless network for IoT, in which all the ground devices are homogeneous PPP distributed in a circular disaster area with radius $\mathcal{R} = 200$ m. The UAV is deployed at the center of the area with height $H = 50$ m. The maximum angle of transmit antennas $\varphi = 60°$. The area is divided into 6 clusters, i.e. $\hat{N} = 6$. The radius of each cluster is 50 m.

A. Number of D2D Hops

To extend the wireless coverage of the UAV, we design the SPR algorithm to select proper nodes and establish the multi-hop D2D links. The simulation results of the minimum number of hops that is needed to establish the multi-hop D2D link in the SPR algorithm is shown in Table I for both uplink and downlink, comparing with the distributed algorithm in [35], when the distance between the source node and destination node $\mathcal{R}$ is varying. In the simulation, we set $\theta = 120°$, $r = 10$ m, $P_{sum} = 10$ mW, and $\lambda_D = 0.001$. σ^2 is set to -110 dBm according to [46], which can be ignored when calculating the outage probability. The available nodes in the cluster is $N = 100$. In addition, to save energy for each device in disasters, the transmit power of each D2D node is assumed to be as low as $\hat{P} = 1$ mW to prolong the battery of each D2D node. From the results, we can know that the SPR algorithm can achieve reliable performance with much less number of D2D nodes, which is very important for the emergency communications in disasters with limited energy supply. In addition, as the distance between the transmitter and receiver of each D2D link is set to be no longer than $r = 10$ m, the minimum number of D2D nodes to connect the source and destination with $\mathcal{R} = 100$ m is 10. From Table I, we can also see that in our proposed SPR algorithm, only 10 D2D nodes and 12 D2D nodes are needed to establish the multi-hop link for the uplink and downlink with $\mathcal{R} = 100$ m, respectively, which is very close to the minimum value of 10. Furthermore, the number of D2D nodes for the downlink is a little larger than that for the uplink, due to the fact that the interference from UAV is considered in the downlink, but not in the uplink.

B. Outage Probability of D2D Links

For the multi-hop D2D link, the relationship between the expected outage probability and the reliable constraint ϕ is demonstrated in Fig. 3, for the uplink and downlink. $P_{sum} = 10$ mW, $\lambda_D = 0.001$, $\hat{P} = 1$ mW, $\varepsilon = -6$ dB, $\sigma^2 = -110$ dBm, and $N = 100$. From the results, we can see that when ϕ_{UL} in (21) or ϕ_{DL} in (22) becomes larger, the outage probability decreases at first, and then, it increases again. According to (25) and (26), when ϕ gets higher, the number of hops becomes larger too, which makes the outage probability become smaller first. However, when ϕ tends to 1, the number of hops tends to be extremely large, which makes

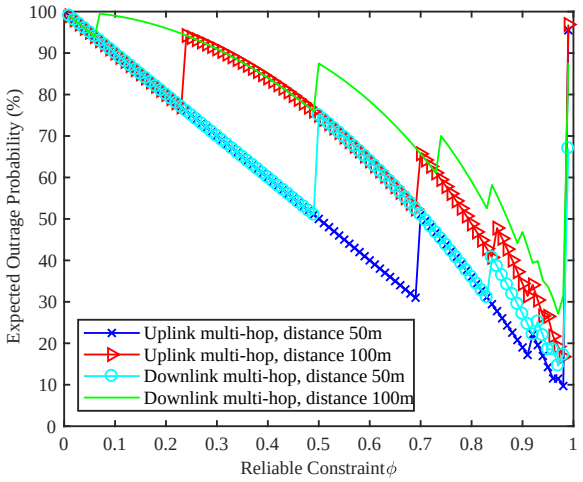

Fig. 3. Relationship between the expected outage probability and the reliable constraint ϕ for the uplink and downlink, with different $\mathcal{R}$ between the source and destination. $P_{sum} = 10$ mW, $\lambda_D = 0.001$, $\hat{P} = 1$ mW, $\varepsilon = -6$ dB, $\sigma^2 = -110$ dBm and $N = 100$.

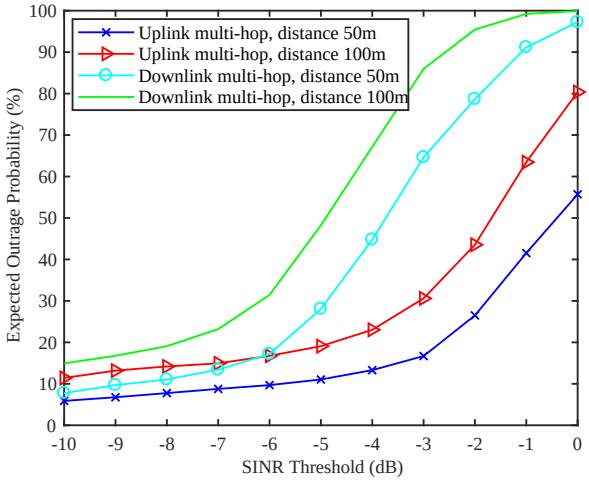

Fig. 4. Comparison of the expected outage probability with different SINR threshold ε for the uplink and downlink. $P_{sum} = 10$ mW $\lambda_D = 0.001$, $\hat{P} = 1$ mW, $\sigma^2 = -110$ dBm, $\phi = 0.98$ and $N = 100$.

the outage probability become larger again. When ϕ is set about 0.98, the outage probability can achieve its minimum. In addition, we can notice that the outage probability becomes larger with increasing $\mathcal{R}$. Furthermore, the outage probability for the downlink is larger than that for the uplink, due to the fact that the interference from UAV is considered in the downlink, but not in the uplink.

In Figs. 4-6, the expected outage probability of the multi-hop D2D link for the uplink and downlink is compared with different values of SINR threshold ε, number of available devices N and transmit power of each device $\hat{P}$, respectively. $P_{sum} = 10$ mW, $\lambda_D = 0.001$, $\sigma^2 = -110$ dBm and $\phi = 0.98$. First, we set $N = 100$ and $\hat{P} = 1$ mW in Fig. 4. From the results, we can see that the outage probability of D2D links becomes larger, when larger SINR threshold ε is set. This is due to the fact that the SINR requirement of each D2D link becomes much more difficult to satisfy when ε is larger. In addition, we can also notice that the outage probability

TABLE I
MINIMUM NUMBER OF D2D HOPS WITH VARYING DISTANCE $\mathcal{R}$

Distance $\mathcal{R}$ (m)	10	20	30	40	50	60	70	80	90	100
Uplink: Number of D2D Hops in SPR Algorithm	1	2	3	4	5	6	7	8	9	10
Downlink: Number of D2D Hops in SPR Algorithm	2	3	4	5	6	8	9	10	11	12
Uplink: Number of D2D Hops in [35]	3	5	7	10	12	15	17	20	22	25
Downlink: Number of D2D Hops in [35]	4	7	9	12	14	17	19	22	24	27

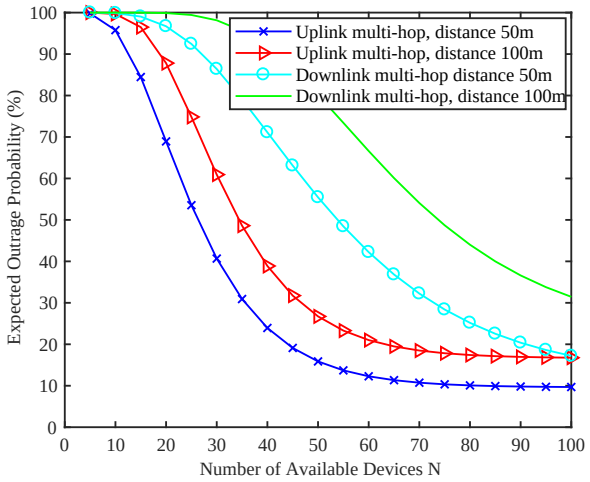

Fig. 5. Comparison of the expected outage probability with different number of available devices N for the uplink and downlink. $P_{sum} = 10$ mW, $\lambda_D = 0.001$, $\varepsilon = -6$ dB, $\hat{P} = 1$ mW, $\sigma^2 = -110$ dBm and $\phi = 0.98$.

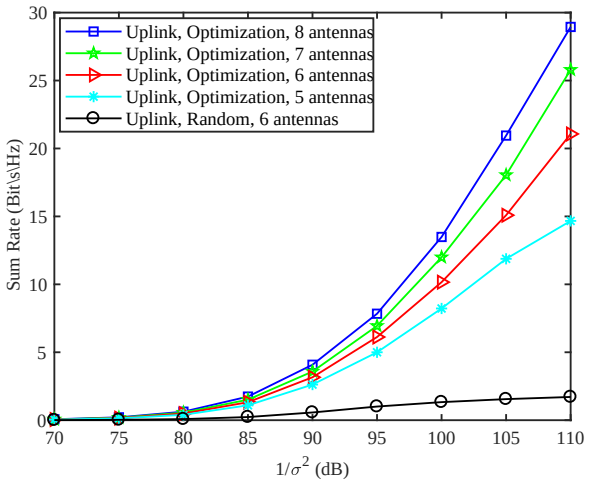

Fig. 7. Sum rate comparison of the optimal transceiver design for the uplink transmission with different antennas equipped at the UAV, when the SNR is varying. 6 ground devices are considered, $\hat{P} = 2$ mW.

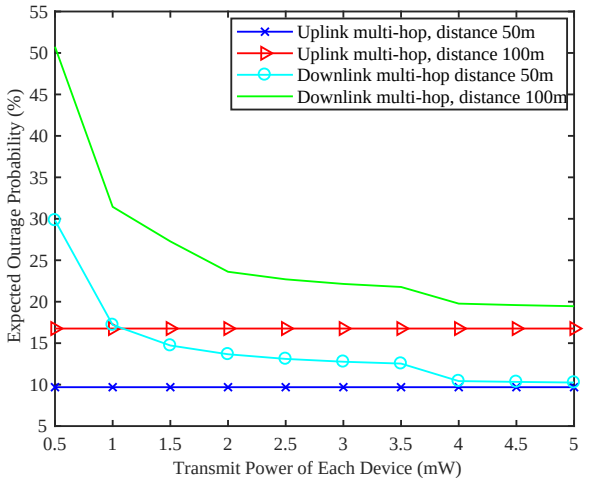

Fig. 6. Comparison of the expected outage probability with different transmit power of each device for the uplink and downlink. $P_{sum} = 10$ mW, $\lambda_D = 0.001$, $\varepsilon = -6$ dB, $\sigma^2 = -110$ dBm, $\phi = 0.98$ and $N = 100$.

becomes larger with increasing $\mathcal{R}$. Then, we set $\varepsilon = -6$ dB and $\hat{P} = 1$ mW in Fig. 5. From the results, we can notice that the outage probability of D2D links becomes lower when there exist more available D2D nodes that can provide service. This is because the multi-hop D2D link becomes more reliable when the relays can be selected from more available devices. Furthermore, we set $\varepsilon = -6$ dB and $N = 100$ in Fig. 6. From the results, we can observe that the outage probability of D2D links becomes lower for the downlink when the transmit power of each D2D node becomes higher, due to the fact that higher transmit power will also result in higher received SINR. On the other hand, for the uplink, the outage probability of D2D links remains unchanged when the transmit power of each D2D node is varying. This is because the interference only comes from the other D2D transmission in the same cluster for the uplink according to (27), whose power will also become larger with larger transmit power of each D2D node. Furthermore, for all the results in Figs. 4-6, the outage probability for the downlink is larger than that for the uplink, due to the fact that the interference from UAV is considered in the downlink, but not in the uplink.

C. Optimal Transceiver Design Schemes of UAV

First, the uplink transmission between the mobile devices and the UAV is analyzed in Fig. 7, in which the sum rate of the proposed optimal transceiver design is compared with different SNR and different number of antennas at the UAV. In the simulation, 6 ground mobile devices are considered, and we set the transmit power of each device $\hat{P} = 2$ mW. From the results, we can see that the proposed scheme can achieve much better performance than that when the decoding vectors are randomly generated. In addition, the reliable performance can be guaranteed only when $M \geq 6$, in which most of the interference can be eliminated. Furthermore, the sum rate will increase when more antennas are equipped at the UAV.

For the downlink, the sum rate of the optimal transceiver design is shown with different value of background noise σ^2 in Fig. 8, respectively. In the simulation, 6 ground devices are considered and $P_{sum} = 10$ mW. From the results, we

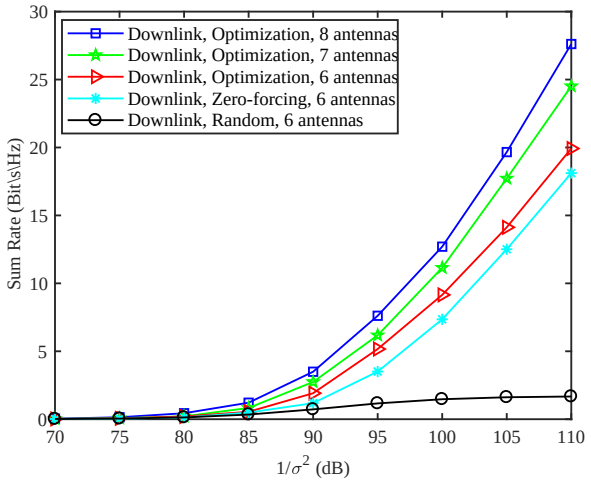

Fig. 8. Sum rate comparison of the optimal transceiver design for the downlink transmission with different number of antennas equipped at the UAV, when the background power is varying. $P_{sum} = 10$ mW.

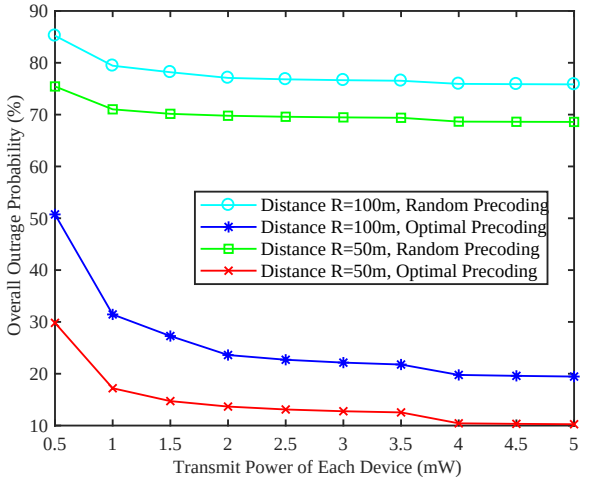

Fig. 9. Overall outage probability comparison of UAV downlink and multi-hop D2D link with different transmit power of each device. $N = 100$, $M = 6$, $\sigma^2 = -110$ dBm, $\varepsilon = -6$ dB and $P_{sum} = 10$ mW.

can observe that the sum rate will increase with lower power of the background noise. In addition, we can also notice that the sum rate will increase with more antennas equipped at the UAV when the optimal transceiver design is performed. Furthermore, when the zero-forcing method is performed with 6 antennas, its performance is a little lower than that of the optimal transceiver design.

D. Overall Outage Probability of the Whole System

In this subsection, the overall outage probability of the whole system is analyzed, i.e., the combination of UAV downlink and multi-hop D2D link. The results of the uplink is similar to that of the downlink, which will not be presented. The overall downlink outage probability is compared in Fig. 9 with different distance from the source D2D node to the destination and different precoding methods, when the transmit power of each device $\hat{P}$ is varying. In the simulation, we set $\sigma^2 = -110$ dBm, $\varepsilon = -6$ dB, $N = 100$, M=6 and $P_{sum} = 10$ mW. From the results, we can know that the overall outage probability can be significantly reduced through the SPR algorithm to establish the multi-hop D2D links and the proposed optimal transceiver design scheme. In addition, we can also notice that the outage probability can be reduced with higher transmit power of each device or shorter distance between the source D2D node and the destination $\mathcal{R}$.

VII. Concluding Remarks

In this paper, the multi-hop D2D and UAV BS have been combined to perform emergency transmission for IoT in disasters. For the multi-hop D2D transmission, the SPR algorithm was designed to construct multi-hop D2D links with the minimum number of hops to enhance the wireless coverage of UAV effectively, which can save energy for the limited batteries of ground devices in disasters. In addition, the outage probability of the multi-hop D2D links for the uplink and downlink was also analyzed. Furthermore, two optimal transceiver design schemes were proposed for the uplink from the ground devices to the UAV and the downlink from the UAV to the devices, respectively, to improve the performance of UAV transmission effectively. To make these two problems for the UAV uplink and downlink much easier to solve, corresponding algorithms with low computational complexity were also proposed. Simulation results were presented to show the effectiveness of our proposed schemes.

References

[1] X. Liu, G. Gui, N. Zhao, W. Meng, Z. Li, Y. Chen, and F. Adachi, "UAV coverage for downlink in disasters: Precoding and multi-hop D2D," in *Proc. IEEE/CIC ICCC'18*, pp. 1–6, Beijing, China, Aug. 2018.

[2] Y. Ran, "Considerations and suggestions on improvement of communication network disaster countermeasures after the wenchuan earthquake," *IEEE Commun. Mag.*, vol. 49, no. 1, pp. 44–47, Jan. 2011.

[3] L. Bai, L. Zhu, X. Zhang, W. Zhang, and Q. Yu, "Multi-satellite relay transmission in 5G: Concepts, techniques and challenges," *IEEE Network*, to appear.

[4] Q. Yu, J. Wang, and L. Bai, "Architecture and critical technologies of space information networks," *J. Commun. Inf. Netw.*, vol. 1, no. 3, pp. 1–9, Sept. 2016.

[5] S. Hayat, E. Yanmaz, and R. Muzaffar, "Survey on unmanned aerial vehicle networks for civil applications: A communications viewpoint," *IEEE Commun. Surveys Tuts.*, vol. 18, no. 4, pp. 2624–2661, Fourthquarter. 2016.

[6] A. A. Khuwaja, Y. Chen, N. Zhao, M.-S. Alouini, and P. Dobbins, "A survey of channel modeling for UAV communications," *IEEE Commun. Surveys Tuts.*, to be published, DOI: 10.1109/COMST.2018.2856587.

[7] N. Zhang, S. Zhang, P. Yang, O. Alhussein, W. Zhuang, and X. S. Shen, "Software defined space-air-ground integrated vehicular networks: Challenges and solutions," *IEEE Commun. Mag.*, vol. 55, no. 7, pp. 101–109, Jul. 2017.

[8] Y. Zeng, R. Zhang, and T. J. Lim, "Wireless communications with unmanned aerial vehicles: Opportunities and challenges," *IEEE Commun. Mag.*, vol. 54, no. 5, pp. 36–42, May. 2016.

[9] J. Lyu, Y. Zeng, R. Zhang, and T. J. Lim, "Placement optimization of UAV-mounted mobile base stations," *IEEE Commun. Lett.*, vol. 21, no. 3, pp. 604–607, Mar. 2017.

[10] Y. Zeng and R. Zhang, "Energy-efficient UAV communication with trajectory optimization," *IEEE Trans. Wireless Commun.*, vol. 16, no. 6, pp. 3747–3760, Jun. 2017.

[11] J. Zhao, F. Gao, Q. Wu, S. Jin, Y. Wu, and W. Jia, "Beam tracking for UAV mounted SatCom on-the-move with massive antenna array," *IEEE J. Sel. Areas Commun.*, to appear.

[12] F. Cheng, S. Zhang, Z. Li, Y. Chen, N. Zhao, F. R. Yu, and V. C. M. Leung, "UAV trajectory optimization for data offloading at the edge of multiple cells," *IEEE Trans. Veh. Technol.*, vol. 67, no. 7, pp. 6732–6736, Jul. 2018.

[13] N. Zhao, F. Cheng, F. R. Yu, J. Tang, Y. Chen, G. Gui, and H. Sari, "Caching UAV assisted secure transmission in hyper-dense networks based on interference alignment," *IEEE Trans. Commun.*, vol. 66, no. 5, pp. 2281–2294, May 2018.

[14] H. Lu, Y. Li, S. Mu, D. Wang, H. Kim, and S. Serikawa, "Motor anomaly detection for unmanned aerial vehicles using reinforcement learning," *IEEE Internet Things J.*, to appear.

[15] Z. Xiao, P. Xia, and X.-G. Xia, "Enabling UAV cellular with millimeter-wave communication: potentials and approaches," *IEEE Commun. Mag.*, vol. 54, no. 5, pp. 66–73, 2016.

[16] C. Yin, Z. Xiao, X. Cao, X. Xi, P. Yang, and D. Wu, "Offline and online search: UAV multi-objective path planning under dynamic urban environment," *IEEE Internet Things J.*, to appear.

[17] Y. Chen, N. Zhao, Z. Ding, and M.-S. Alouini, "Multiple UAVs as relays: Multi-hop single link versus multiple dual-hop links," *IEEE Trans. Wireless Commun.*, vol. 17, no. 9, pp. 6348–6359, Sept. 2018.

[18] H. Wu, X. Tao, N. Zhang, and X. S. Shen, "Cooperative UAV cluster assisted terrestrial cellular networks for ubiquitous coverage," *IEEE J. Sel. Areas Commun.*, to appear.

[19] J. Zhao, F. Gao, L. Kuang, Q. Wu, and W. Jia, "Channel tracking with flight control system for UAV mmWave MIMO communications," *IEEE Commun. Lett.*, vol. 22, no. 6, pp. 1224–1227, Jun. 2018.

[20] Q. Yu, C. Han, L. Bai, J. Choi, and X. Shen, "Low-complexity multiuser detection in millimeter-wave systems based on opportunistic hybrid beamforming," *IEEE Trans. Veh. Technol.*, to appear.

[21] M. Erdelj and E. Natalizio, "UAV-assisted disaster management: Applications and open issues," in *Proc. ICNC'16*, pp. 1–5, Kauai, Hawaii, Feb. 2016.

[22] K. Mase and H. Okada, "Message communication system using unmanned aerial vehicles under large-scale disaster environments," in *Proc. IEEE PIMRC'15*, pp. 2171–2176, Hong Kong, China, Aug. 2015.

[23] D. G. Reina, S. L. Toral, and H. Tawfik, "UAVs deployment in disaster scenarios based on global and local search optimization algorithms," in *Proc. DeSE'16*, pp. 197–202, Liverpool, UK, Aug. 2016.

[24] E. Christy, R. P. Astuti, B. Syihabuddin, B. Narottama, O. Rhesa, and F. Rachmawati, "Optimum UAV flying path for device-to-device communications in disaster area," in *Proc. ICSigSys'16*, pp. 318–322, Sanur, Indonesia, May 2017.

[25] L. Wei, R. Hu, Y. Qian, and G. Wu, "Enable device-to-device communications underlaying cellular networks: challenges and research aspects," *IEEE Commun. Mag.*, vol. 52, no. 6, pp. 90–96, Jun. 2014.

[26] M. Li, L. Bai, Q. Yu, and J. Choi, "Optimal beamforming for dual-hop MIMO AF relay networks with imperfect CSI," *IET Commun.*, vol. 12, no. 2, pp. 115–124, Feb. 2018.

[27] M. Li, L. Bai, Q. Yu, and J. Choi, "Optimal beamforming for dual-hop MIMO AF relay networks with cochannel interferences," *IEEE Trans. Signal Process.*, vol. 65, no. 7, pp. 1825–1840, Apr. 2017.

[28] Z. Li, L. Guan, C. Li, and A. Radwan, "A secure intelligent spectrum control strategy for future THz mobile heterogeneous networks," *IEEE Commun. Mag.*, vol. 56, no. 6, pp. 116–123, Jun. 2018.

[29] Y. Cao, N. Zhao, F. R. Yu, M. Jin, Y. Chen, J. Tang, and V. C. M. Leung, "Optimization or alignment: Secure primary transmission assisted by secondary networks," *IEEE J. Select. Areas Commun.*, vol. 36, no. 4, pp. 905–917, Apr. 2018.

[30] W. Feng, Y. Wang, and D. Lin, "When mmWave communications meet network densification: a scalable interference coordination perspective," *IEEE J. Select. Areas Commun.*, vol. 35, no. 7, pp. 1459–1471, Jul. 2017.

[31] H. Nishiyama, M. Ito, and N. Kato, "Relay-by-smartphone: realizing multihop device-to-device communications," *IEEE Commun. Mag.*, vol. 52, no. 4, pp. 56–65, Apr. 2014.

[32] D. Feng, L. Lu, Y. Y. Wu, G. Y. Li, G. Feng, and S. Li, "Device-to-device communications underlaying cellular networks," *IEEE Trans. Commun.*, vol. 61, no. 8, pp. 3541–3551, Aug. 2013.

[33] X. Lin, J. G. Andrews, and A. Ghosh, "Spectrum sharing for device-to-device communication in cellular networks," *IEEE Trans. Wireless Commun.*, vol. 13, no. 12, pp. 6727–6740, Dec. 2014.

[34] D. Wu, J. Wang, R. Q. Hu, Y. Cai, and L. Zhou, "Energy-efficient resource sharing for mobile device-to-device multimedia communications," *IEEE Trans. Veh. Technol.*, vol. 63, no. 5, pp. 2093–2103, Jun. 2014.

[35] T. Ban and B. C. Jung, "On the link scheduling for cellular-aided device-to-device networks," *IEEE Trans. Veh. Technol.*, vol. 65, no. 11, pp. 9404–9409, Nov. 2016.

[36] J. Li, M. Liu, J. Lu, F. Shu, Y. Zhang, S. Bayat, and D. N. K. Jayakody, "On social-aware content caching for D2D-enabled cellular networks with matching theory," *IEEE Internet Things J.*, to appear.

[37] Z. Zhou, M. Dong, K. Ota, G. Wang, and L. T. Yang, "Energy-efficient resource allocation for D2D communications underlaying cloud-RAN-based LTE-A networks," *IEEE Internet Things J.*, vol. 3, no. 3, pp. 428–438, Jun. 2016.

[38] Y. He, F. R. Yu, N. Zhao, and H. Yin, "Secure social networks in 5G systems with mobile edge computing, caching and device-to-device communications," *IEEE Wireless Commun.*, vol. 25, no. 3, pp. 103–109, Jun. 2018.

[39] H. Mao, W. Feng, and N. Ge, "Performance of social-position relationships based cooperation among mobile terminals," *IEEE Trans. Veh. Technol.*, vol. 65, no. 5, pp. 3128–3138, May. 2016.

[40] N. Cheng, N. Lu, N. Zhang, T. Yang, X. Shen, and J. W. Mark, "Vehicle-assisted device-to-device data delivery for smart grid," *IEEE Trans. Veh. Technol.*, vol. 65, no. 4, pp. 2325–2340, Apr. 2016.

[41] Z. Xiao, L. Zhu, J. Choi, P. Xia, and X. Xia, "Joint power allocation and beamforming for non-orthogonal multiple access (NOMA) in 5G millimeter wave communications," *IEEE Trans. Wireless Commun.*, vol. 17, no. 5, pp. 2961–2974, May 2018.

[42] H. S. Jo, Y. J. Sang, P. Xia, and J. G. Andrews, "Heterogeneous cellular networks with flexible cell association: A comprehensive downlink SINR analysis," *IEEE Trans. Wireless. Commun.*, vol. 11, no. 10, pp. 3484–3495, Oct. 2012.

[43] Z. Zong, H. Feng, F. R. Yu, N. Zhao, T. Yang, and B. Hu, "Optimal transceiver design for SWIPT in K-user MIMO interference channels," *IEEE Trans. Wireless. Commun.*, vol. 15, no. 1, pp. 430–445, Jan. 2016.

[44] A. J. Smola, S. V. N. Vishwanathan, and T. Hofmann, "Kernel methods for missing variables," in *Proc. AISTATS'05*, pp. 325–332, Barbados, Jan. 2005.

[45] M. S. Lobo, L. Vandenberghe, S. Boyd, and H. Lebret, "Applications of second-order cone programming," *Linear Algebra Appl.*, vol. 284, no. 1-3, pp. 193–228, Nov. 1998.

[46] Y. Zeng, X. Xu, and R. Zhang, "Trajectory design for completion time minimization in UAV-enabled multicasting," *IEEE Trans. Wireless Commun.*, vol. 17, no. 4, pp. 2233–2246, 2018.

Xiaonan Liu received the B.E. degree from Dalian University of Technology, Dalian, China, in 2016, where he is currently pursuing the M.E. degree with the School of Information and Communication Engineering. His current research interests include UAV communications, interference alignment, cache-aided networks, NOMA and deep learning.

Zan Li (M'06-SM'14) received her B.S. degree in communications engineering and her M.S. and Ph.D. degrees in communication and information systems from Xidian University, Xian, China, in 1998, 2000, and 2004, respectively. She is currently a professor with the State Key Laboratory of Integrated Services Networks, School of Telecommunications Engineering, Xidian University. Her research interests include wireless communication and signal processing, particularly covert communication, weak signal detection, spectrum sensing, and cooperative communication.

Nan Zhao (S'08-M'11-SM'16) is currently an Associate Professor at Dalian University of Technology, China. He received the Ph.D. degree in information and communication engineering in 2011, from Harbin Institute of Technology, Harbin, China.

Dr. Zhao is serving or served on the editorial boards of 7 SCI-indexed journals, including IEEE Transactions on Green Communications and Networking. He won the best paper awards in IEEE VTC 2017 Spring, MLICOM 2017, ICNC 2018 and CSPS 2018. He also received the IEEE Communications Society Asia Pacific Board Outstanding Young Researcher Award in 2018.

Weixiao Meng (SM'10) received the B.Eng., M. Eng., and Ph.D. degrees from Harbin Institute of Technology (HIT), Harbin, China, in 1990, 1995, and 2000, respectively. From 1998 to 1999, he worked at NTT DoCoMo on adaptive array antenna and dynamic resource allocation for beyond 3G as a senior visiting researcher. He is now a full professor and the vice dean of the School of Electronics and Information Engineering of HIT. His research interests include broadband wireless communications and networking, MIMO, GNSS receiver and wireless localization technologies. He has published 4 books and over 260 papers on journals and international conferences. He is the Chair of IEEE Communications Society Harbin Chapter, a Fellow of the China Institute of Electronics, a senior member of the IEEE ComSoc and the China Institute of Communication. He has been an editorial board member for Wileys WCMC Journal since 2010, an area editor for PHYCOM journal since 2014, an editorial board for IEEE Communications Surveys and Tutorials since 2014 and IEEE Wireless Communications since 2015. He acted as leading TPC co-chair of ChinaCom2011 and ChinaCom2016, leading Services and Applications track co-chair of IEEE WCNC2013, Awards co-chair of IEEE ICC2015 and Wireless Networking Symposia co-Chair of IEEE Globecom2015, AHSN Symposia co-Chair of IEEE Globecom2018, Workshop co-Chair of IEEE ICC2019. In 2005 he was honored provincial excellent returnee and selected into New Century Excellent Talents (NCET) plan by Ministry of Education, China in 2008, and the Distinguished Academic Leadership of Harbin.

Guan Gui received the Dr. Eng. degree in information and communication engineering from University of Electronic Science and Technology of China (UESTC), Chengdu, China, in 2011. From October 2009 to March 2014, he joined Tohoku University as for research assistant as well as postdoctoral research fellow, respectively. From April 2014 to October 2015, he was an Assistant Professor in Akita Prefectural University. Since November 2015, he has been a professor with Nanjing University of Posts and Telecommunications (NJUPT), Nanjing, China. He is currently engaged in research of deep learning, compressive sensing, and advanced wireless techniques. He is a senior member of Institute of Electrical and Electronics Engineers (IEEE). Dr. Gui has been serving editors of Security and Communication Networks (2012-2016), IEEE Transactions on Vehicular Technology (2017-), IEEE Access (2018-) and KSII Transactions on Internet and Information Systems (2017-). He received several best paper awards such as ICC2014, ICC2017 and VTC2014-Spring.

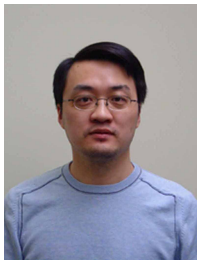

Yunfei Chen (S'02-M'06-SM'10) received his B.E. and M.E. degrees in electronics engineering from Shanghai Jiaotong University, Shanghai, P.R.China, in 1998 and 2001, respectively. He received his Ph.D. degree from the University of Alberta in 2006. He is currently working as an Associate Professor at the University of Warwick, U.K. His research interests include wireless communications, cognitive radios, wireless relaying and energy harvesting.

Fumiyuki Adachi (M'79-SM'90-F'02-LF'16) received the B.S. and Dr. Eng. degrees in electrical engineering from Tohoku University, Sendai, Japan, in 1973 and 1984, respectively. In April 1973, he joined the Electrical Communications Laboratories of Nippon Telegraph & Telephone Corporation (now NTT) and conducted research on digital cellular mobile communications. From July 1992 to December 1999, he was with NTT DOCOMO, where he led a research group on wideband/broadband wireless access for 3G and beyond. He contributed to the development of 3G air interface standard, known as W-CDMA. Since January 2000, he has been with Tohoku University, Sendai, Japan. He was a full professor at the Dept. of Communications Engineering of the Graduate School of Engineering until March 2016. Currently He is a Specially Appointed Professor for Research at the Research Organization of Electrical Communication (ROEC) and is leading a wireless signal processing research group aiming at 5G systems and beyond. His research interests are in the area of wireless signal processing and networking, including multi-access, equalization, antenna diversity, adaptive transmission, channel coding, radio resource management, etc. From October 1984 to September 1985, he was a United Kingdom SERC Visiting Research Fellow in the Department of Electrical Engineering and Electronics at Liverpool University.

Dr. Adachi is an IEEE Life Fellow and an IEICE Fellow. He is a recipient of the IEEE Vehicular Technology Transactions Best Paper of the Year Award 1980 and 1990, the IEICE Transactions Best Paper of the Year Award 1996, 1998 and again 2009, IEEE VTS Avant Garde award 2000, IEICE Achievement Award 2002, IEEE VTS Conference Chair Award 2014, IEEE VTS Conference Chair Award 2014, and IEEE VTS Stuart Meyer Memorial Award 2017 and IEEE ComSoc RCC Technical Recognition Award 2017. He is also a recipient of Thomson Scientific Research Front Award 2004, Ericsson Telecommunications Award 2008, Telecom System Technology Award 2009, Prime Minister Invention Prize 2010, British Royal Academy of Engineering Distinguished Visiting Fellowship 2011, KDDI Foundation Research Award 2012, C&C Prize 2014, Rinzaburo Shida Award 2016, Sendai Municipal Commendation 2017, IEEE VTS Stuart Meyer Memorial Award 2017, and IEEE ComSoc RCC Technical Recognition Award 2017. He is listed in Highly Cited Researchers 2001 (http://hcr.stateofinnovation.thomsonreuters.com/page/archives).